Seasonal and interannual variations in atmospheric oxygen and implications for the global carbon cycle

Ralph F. Keeling & Stephen R. Shertz

National Center for Atmospheric Research, PO Box 3000, Boulder, Colorado 80307-3000, USA

Measurements of changes in atmospheric molecular oxygen using a new interferometric technique show that the O_2 content of air varies seasonally in both the Northern and Southern Hemispheres and is decreasing from year to year. The seasonal variations provide a new basis for estimating global rates of biological organic carbon production in the ocean, and the interannual decrease constrains estimates of the rate of anthropogenic CO_2 uptake by the oceans.

THE dominant processes influencing the abundance of atmospheric O_2 on timescales less than many thousands of years are chemical reactions involving the creation and destruction of organic matter: that is, photosynthesis, respiration and combustion. These reactions cause atmospheric O_2 to vary inversely with atmospheric CO_2 with an O_2 : C exchange ratio that depends on the composition of the organic matter. Additional chemical reactions, however, influence the abundance of atmospheric CO_2. The difference in the geochemistry of O_2 and CO_2 arises because, whereas dissolved O_2 is chemically neutral, dissolved CO_2 reacts with water to form carbonic acid, which in turn reacts with basic compounds such as carbonates. As a result of the differing acid-base properties of O_2 and CO_2, measurements of changes in atmospheric O_2 can constrain aspects of the global carbon cycle that are not constrained by measurements of atmospheric CO_2 alone.

Consider, for example, the processes controlling the increase in atmospheric CO_2 over the past century. The dominant sources of CO_2 are fossil-fuel burning and carbon releases associated with land-use changes while the dominant sinks may involve a combination of oceanic uptake and uptake by terrestrial ecosystems[1,2]. With one exception, these sources and sinks of CO_2 are stoichiometrically linked to sources and sinks of O_2. The exception is the uptake of CO_2 by the oceans which essentially proceeds through the reaction of dissolved CO_2 with carbonate ions and therefore does not involve O_2 (ref. 3). Thus, in principle, the difference between the decrease in atmospheric O_2, corrected for reaction stoichiometry, and the increase in atmospheric CO_2 can determine the uptake of CO_2 by physical dissolution in the oceans.

The acid-base chemistry of CO_2 also leads to qualitative differences in the fluxes of O_2 and CO_2 across the air-sea interface that are driven by marine biological processes. Marine photosynthesis and respiration produce comparable changes (in mol m^{-3}) in dissolved O_2 and total dissolved inorganic carbon in sea water. Changes in dissolved CO_2 gas are ~15 times smaller, however, as determined by the chemical equilibrium between dissolved CO_2 gas and the other (dominant) forms of dissolved inorganic carbon, especially bicarbonate and carbonate ions[3,24]. Because air-sea gas fluxes tend to be driven in proportion to the saturation anomalies in dissolved gas concentrations[4], biologically induced air-sea fluxes of CO_2 are ~15 times smaller than fluxes of O_2 (ref. 5). Other important qualitative differences in the behaviour of CO_2 and O_2 arise because the equilibration timescale for dissolved CO_2 is ~15 times longer (~1 year) than that of dissolved O_2 (a few weeks)[3,5].

Observed variations in atmospheric oxygen

Previous attempts to measure changes in the percentage of atmospheric O_2 in background air were thwarted by the high O_2 content of air[6,7]. Here we report measurements using a new interferometric technique[8,9] which overcomes that limitation.

We detect oxygen changes through changes in the O_2/N_2 ratio of air samples. Because atmospheric N_2 is believed to be much less variable than O_2, changes in the O_2/N_2 ratio should primarily reflect changes in O_2 (ref. 8). Changes in O_2/N_2 are reported as relative deviations from a reference

$$\delta(O_2/N_2) = \left(\frac{(O_2/N_2)_{sample}}{(O_2/N_2)_{ref.}} - 1 \right) \quad (1)$$

We propose the convention of multiplying $\delta(O_2/N_2)$ by 10^6 and expressing the result in units of 'per meg'. In these units $1/0.2095 = 4.8$ per meg is equivalent to 1 p.p.m. by volume (p.p.m.v) because O_2 comprises 20.95% of air by volume[7].

Our reference for the O_2/N_2 determinations is based on the average composition of the air derived from a suite of six high-pressure cylinders. The O_2/N_2 ratios of flask samples are determined first relative to a working gas. We compare the working gas frequently with a pair of secondary reference gases which, in turn, are compared at roughly six-month intervals with the six primary reference gases. These primary reference gases have shown detectable changes relative to each other but no systematic trends over a period of four years.

External precision, based on analysis of replicate flasks, is roughly ±4 per meg. Additional uncertainty must be allowed, however, for day-to-day variations in O_2/N_2 ratio of the air delivered from the reference gas cylinders. Allowing for this variability, we estimate the overall precision of the average concentration of the replicate flasks to be ±6 per meg relative to the long-term mean composition of the air delivered from the primary reference cylinders.

Results from samples collected at three sea-level sites, Alert, Ellesmere Island (82.5° N, 62.3° W), La Jolla, California (32.9° N, 117.3° W) and Cape Grim, Tasmania (40.7° S, 114.7° E) are shown in Fig. 1. Significant seasonal variations in $\delta(O_2/N_2)$ occur at all three sites. An interannual decrease in O_2/N_2 is clearly evident in the La Jolla data. As discussed below, the decrease rate is consistent with the global rate of O_2 consumption from the burning of fossil fuels. Oxygen depletion from burning fossil fuels is not a serious environmental concern because the changes are minuscule compared with the total O_2 abundance in air[10].

Interpretation of seasonal variations

At the two Northern Hemisphere sites, the seasonal variations in O_2/N_2 are strongly anticorrelated with variations in CO_2. The amplitude of the O_2/N_2 cycle is larger than would be expected from the CO_2 variations. The CO_2 cycle is known to

be caused primarily by seasonal uptake and release of CO_2 by land plants and soils[11]. Taking an average O_2:CO_2 exchange ratio for the formation and destruction of terrestrial organic matter of −1.05:1 (ref. 8), we estimate that $\delta(O_2/N_2)$ should increase by 5 per meg for each 1 p.p.m. decrease in CO_2 over the seasonal cycle. Instead, the observed ratio at the Northern Hemisphere sites is closer to 10 per meg per p.p.m. At Cape Grim in the Southern Hemisphere, the O_2/N_2 cycle is even more remarkable with a ~96 per meg seasonal variation in $\delta(O_2/N_2)$ occurring in the presence of a very small (~1 p.p.m.) variation in CO_2.

In addition to exchanges with terrestrial ecosystems, there are two processes that can contribute significantly to seasonal variations in O_2/N_2. First, the amount of O_2 that is dissolved in the upper ocean varies seasonally as the water warms and cools. Because O_2 in upper ocean equilibrates rapidly with the atmosphere, we can estimate the air-sea flux of O_2 associated with seasonal temperature changes from the relation[5]

$$F_{O_2} = -\frac{dC_{eq}}{dT}\frac{\dot{Q}}{C_P} \quad (2)$$

where F_{O_2} is the net O_2 flux (positive into the air) in mol m^{-2} s^{-1}, dC_{eq}/dT is the temperature derivative of the O_2 solubility (mol m^{-3} K^{-1}), $\dot{Q}$ is the rate of change of heat storage in the upper ocean (J m^{-2} s^{-1}) and C_P is the heat capacity of sea water (J m^{-3} K^{-1}). The effect of these fluxes on the atmospheric O_2/N_2 ratio is reduced by ~44% due to a thermally driven flux of N_2 (ref. 5) which we can estimate by applying equation (2) to N_2.

Second, there is net production of O_2 in the euphotic zone (roughly the upper 100 m of the ocean), where, on average, gross photosynthesis exceeds gross respiration, and there is a net consumption of O_2 below the euphotic zone by respiration. Both the net O_2 production rate in the euphotic zone and the rate of vertical mixing between the euphotic zone and deeper waters undergo large seasonal variations. At middle and high latitudes the highest production rates tend to occur in the spring and summer when the waters above 100 m are well stratified[24,25]. A considerable fraction of the O_2 produced at this time escapes into the atmosphere. Comparable amounts of O_2 are removed from the atmosphere in the autumn and winter when stratification breaks down and oxygen-depleted waters from below 100 m depth are brought back into contact with the surface. The air-sea O_2 fluxes associated with this seasonal cycle are linked to the rate at which organic material is produced and exported from the euphotic zone[5,12].

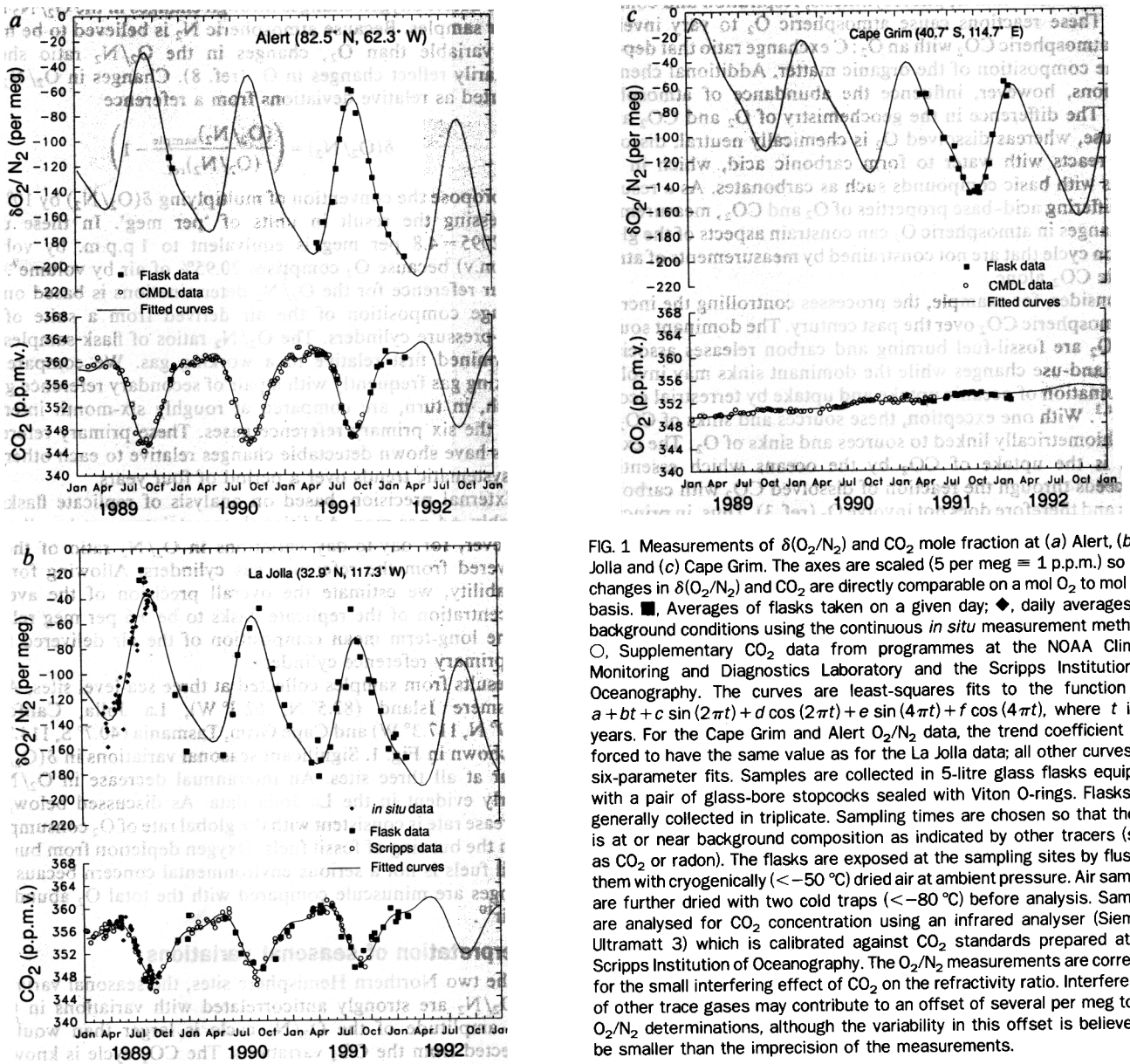

FIG. 1 Measurements of $\delta(O_2/N_2)$ and CO_2 mole fraction at (*a*) Alert, (*b*) La Jolla and (*c*) Cape Grim. The axes are scaled (5 per meg ≡ 1 p.p.m.) so that changes in $\delta(O_2/N_2)$ and CO_2 are directly comparable on a mol O_2 to mol CO_2 basis. ■, Averages of flasks taken on a given day; ◆, daily averages for background conditions using the continuous *in situ* measurement method[9]. ○, Supplementary CO_2 data from programmes at the NOAA Climate Monitoring and Diagnostics Laboratory and the Scripps Institution of Oceanography. The curves are least-squares fits to the function $X = a + bt + c\sin(2\pi t) + d\cos(2\pi t) + e\sin(4\pi t) + f\cos(4\pi t)$, where t is in years. For the Cape Grim and Alert O_2/N_2 data, the trend coefficient b is forced to have the same value as for the La Jolla data; all other curves are six-parameter fits. Samples are collected in 5-litre glass flasks equipped with a pair of glass-bore stopcocks sealed with Viton O-rings. Flasks are generally collected in triplicate. Sampling times are chosen so that the air is at or near background composition as indicated by other tracers (such as CO_2 or radon). The flasks are exposed at the sampling sites by flushing them with cryogenically (<−50 °C) dried air at ambient pressure. Air samples are further dried with two cold traps (<−80 °C) before analysis. Samples are analysed for CO_2 concentration using an infrared analyser (Siemens Ultramatt 3) which is calibrated against CO_2 standards prepared at the Scripps Institution of Oceanography. The O_2/N_2 measurements are corrected for the small interfering effect of CO_2 on the refractivity ratio. Interferences of other trace gases may contribute to an offset of several per meg to the O_2/N_2 determinations, although the variability in this offset is believed to be smaller than the imprecision of the measurements.

Marine photosynthesis and respiration as well as changes in surface water temperature also produce variations in the CO_2 partial pressure of surface waters. The air-sea CO_2 exchange driven biologically is heavily suppressed, however, by the inorganic chemistry of CO_2 in sea water, as mentioned above. The thermal effects on p_{CO_2} are comparable in magnitude and generally opposite in sign to the biological effects, thus leading to even smaller seasonal air-sea CO_2 fluxes than would be expected from either marine biology processes or thermal processes alone[13]. In contrast, the thermal effects and biological effects on O_2 tend to reinforce each other as both lead to higher O_2 supersaturations in the warmer months[12].

In the Northern Hemisphere, we can use the seasonal variations in CO_2, which largely reflect terrestrial exchange, to correct for the effects of terrestrial exchange on the O_2/N_2 variations, thus deriving the residual O_2/N_2 variations attributable to the oceanic exchanges alone (Fig. 2). In the Southern Hemisphere, the lack of a large seasonal variation in CO_2 indicates that the O_2/N_2 variations are almost entirely of marine origin.

The amplitude of the oceanic component of the O_2/N_2 variations within each hemisphere is closely related to the total seasonal net outgassing (SNO) of O_2 in that hemisphere. Here SNO is defined as the areally and temporally integrated flux of O_2 from the ocean into the atmosphere where the time integration extends over the seasonal period when the areally integrated flux is directed into the atmosphere. The close relationship between SNO and the seasonal O_2/N_2 variations follows because the timescale for seasonal variations ($t_{season} \approx 1$ year$/2\pi = 66$ days) is short relative to the timescale for atmospheric interhemispheric exchange ($t_{exch} \approx 1.1$ years[2]) but longer than the timescale for tropospheric mixing within each hemisphere ($t_{hem} \approx 30$ to 60 days). Here we construct preliminary estimates of SNO for the Northern and Southern Hemispheres (Table 1) by assuming that the seasonal amplitudes in O_2/N_2 at the surface are equivalent to what would be achieved if the surface O_2 fluxes were homogeneously diluted into an air mass equal to 50% of the air mass in each hemisphere. This level of atmospheric mixing is consistent with mixing rates for atmospheric CO_2 in the Northern Hemisphere based on recent two- and three-dimensional transport models calibrated with other tracers[11,14].

The estimate of SNO derived in this way includes both biological and thermal components. The thermal component, however, includes only the excess O_2 flux not compensated for by the thermal N_2 flux because only the uncompensated O_2 flux can change the observed O_2/N_2 ratio. The uncompensated thermal component can be estimated independently by applying equation (2) to O_2 and N_2, and thus the biological component can be derived by subtraction. The results (Table 1) indicate that uncompensated thermal degassing accounts for only ~15% of the oceanic component of the O_2/N_2 variations; the remaining 85% is evidently of marine biological origin.

What do these oxygen fluxes tell us about the rates of biological productivity in the ocean? To answer this question it is useful to introduce the concept of net euphotic zone production (NEZP), defined as the net community production (gross production of autotrophs less the gross respiration of autotrophs and heterotrophs) integrated over the depth of the euphotic zone. NEZP may be defined with respect to either organic carbon or O_2. If we accept that net community production of carbon or O_2 requires inputs of 'new' nutrients, then NEZP may be roughly equated with the concept of 'new' production as given in ref. 15. We prefer to express our results in terms of NEZP because the concept of 'new' production of organic matter or O_2 becomes ambiguous whenever organic matter is formed with varying C : N or O_2 : N ratios, or whenever significant nitrification occurs in the euphotic zone.

Areally and annually integrated NEZP of O_2 can be related

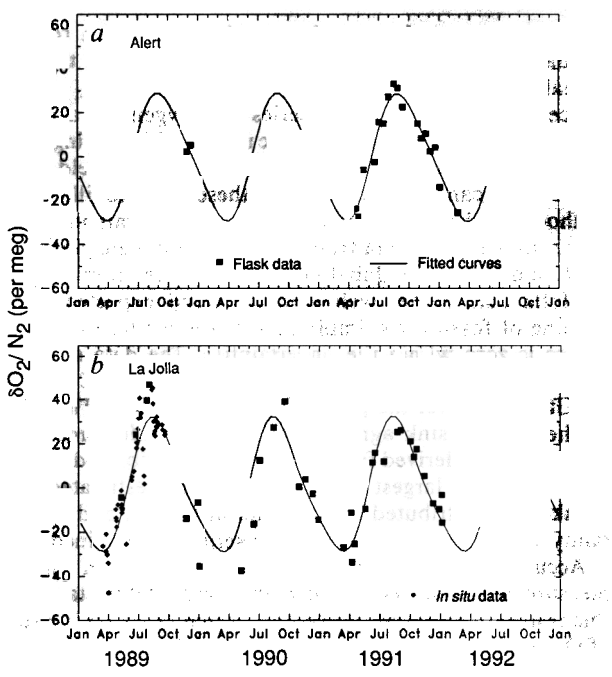

FIG. 2 Detrended oceanic components of the O_2/N_2 variations at Alert (*a*) and La Jolla (*b*). The oceanic component was derived according to $\delta(O_2/N_2)_{oceanic} = \delta(O_2/N_2) + (1.05/0.2095)X_{CO_2}$ where 1.05 is the adopted $-O_2$:CO_2 ratio for exchanges with terrestrial ecosystems, 0.2095 is the O_2 mole fraction of dry air (1/0.2095 is the appropriate conversion factor between per meg units and mole fraction units) and X_{CO_2} is the CO_2 mole fraction in p.p.m. The curve is a least-squares fit of the $\delta(O_2/N_2)_{oceanic}$ data to the same functional form as was used in Fig. 1. The $\delta(O_2/N_2)_{oceanic}$ data and the fitted curve were detrended by subtracting the function $a + bt$, where a and b are the coefficients from the six-parameter fit.

TABLE 1 Components of seasonal variations in oxygen

	Northern Hemisphere	Southern Hemisphere
Total seasonal amplitude	120 per meg*	95 per meg†
Oceanic component of seasonal amplitude	59 per meg‡	85 per meg§
Total SNO‖	5.5×10^{14} mol O_2	7.8×10^{14} mol O_2
Excess thermal component of SNO¶	0.84×10^{14} mol O_2	0.97×10^{14} mol O_2
Biological component of SNO#	4.6×10^{14} mol O_2	6.8×10^{14} mol O_2

* Estimated from the average of the peak-to-peak amplitudes for the fitted curves for the La Jolla and Alert data shown in Fig. 1.

† Estimated from the peak-to-peak amplitude of the fitted curve for the Cape Grim data in Fig. 1.

‡ Estimated from the average of the peak-to-peak amplitudes for the fitted curves for the La Jolla and Alert data shown in Fig. 2.

§ Assumes that the terrestrial exchanges can account for 10 per meg of the seasonal variations at Cape Grim, on the basis of a modelling study for CO_2 at 41° S, 175° E by Heimann *et al.*[11].

‖ Calculated assuming that the surface fluxes are effectively diluted into a volume containing 4.4×10^{19} mol of dry air (50% of the dry air mass in the hemisphere).

¶ Estimated from equation (2) using ocean heat-storage data of Samuels and Cox[21] and solubility data of Weiss[22] (see ref. 5). The reported O_2 flux has been reduced by 46% to account for the compensating flux of N_2. In other words, the reported flux accounts only for the excess O_2 flux not compensated by N_2.

\# Calculated by subtracting the uncompensated thermal component of SNO from total SNO. The biological and thermal components of the SNO should be largely in phase with each other[5].

to biological SNO as follows

$$\mathrm{SNO} = g\ \mathrm{NEZP} \qquad (3)$$

where g is a dimensionless number between 0 and 1.0. g is less than unity because only a fraction of the net O_2 produced throughout the year is reflected in the spring-summer pulse of O_2 injected into the atmosphere: some O_2 is produced in autumn and winter when the net flux is directed into the ocean, and some of the summertime O_2 production is exported into the oxygen-depleted water below the euphotic zone rather than into the atmosphere. In general, we expect middle and high latitudes to dominate the hemispheric SNO, whereas low, middle and high latitudes should all contribute significantly to hemispheric NEZP. We expect that upwelling regions, where O_2 fluxes are generally into the ocean throughout the year but where productivity is high, will reduce hemispheric SNO but make positive contributions to hemispheric NEZP. At present, the uncertainty in g makes it difficult to relate our oxygen signals directly to NEZP. For preliminary estimates, we will adopt $g = 0.5$ for the hemispherically averaged fluxes. This value seems plausible considering that the hemispheric average must include low-latitude waters, where seasonal outgassing is minimal, as well as middle- and high-latitude waters where a significant fraction, probably greater than 50%, of the annual net O_2 production is reflected in the seasonal outgassing[12,16].

Taking $g = 0.5$, the above estimates for SNO lead to estimates of 9.2×10^{14} and 13.6×10^{14} mol O_2 yr^{-1} for NEZP for the Northern and Southern Hemispheres, respectively, or 22.8×10^{14} mol O_2 for the world as a whole. Taking an O_2:C ratio of -1.4:1 (ref. 17) for marine organic matter, we obtain an estimate of 16×10^{14} mol C yr^{-1} (19 gigatonne C yr^{-1}) for global NEZP of organic carbon, or 4 mol C m^{-2} yr^{-1} for the global average. This result is higher than recent estimates of global new production (4–17 Gt C yr^{-1})[18–20] but generally agrees with local estimates derived from observations of O_2 in the upper ocean[12].

The preliminary nature of this analysis must be emphasized: uncertainties in estimated productivities are probably a factor of two or more. Measurements from additional stations are needed to characterize more accurately the large-scale variability in O_2/N_2. More accurate account of atmospheric transport and of the relation between oxygen fluxes and marine productivity is also needed (see also ref. 5). Nevertheless, these results illustrate the contribution that atmospheric O_2 measurements can make to studies of biological activity in the ocean. Measurements of the seasonal variations in O_2/N_2 extending over many years could provide an index of interannual variations in marine productivity on large spatial scales. Such data would be valuable for monitoring the sensitivity of marine productivity to climate change, decreasing stratospheric ozone, eutrophication or other perturbations.

Interpretation of interannual decrease

Schematically, we can represent the global budget for atmospheric CO_2 according to

$$\Delta CO_2 = F + C - O + B \qquad (4)$$

where ΔCO_2 is the annual averaged change in atmospheric CO_2, F is the source of CO_2 from burning fossil fuels, C is the CO_2 source from cement manufacturing, O is the oceanic CO_2 sink, and B is the net source of CO_2 from terrestrial ecosystems (B can be positive or negative), all in units of mol yr^{-1}. Likewise, we can represent the budget for atmospheric oxygen according to

$$\Delta O_2 = -F - H - \alpha_B B \qquad (5)$$

where ΔO_2 is the change in atmospheric oxygen, H is the O_2 sink owing to the oxidation of elements other than carbon (predominantly hydrogen) in fossil fuels and α_B represents the O_2:C exchange ratio for terrestrial biomatter. The oceans do not significantly buffer the decrease in atmospheric O_2 because of the low solubility of O_2 in sea water[8].

TABLE 2 Terms in global O_2 and CO_2 budgets

Symbol	Description	Value around 1990 (10^{14} mol yr^{-1})
Observed quantities		
$-\Delta O_2$	Measured O_2 depletion rate*	6.7 ± 1.7
ΔCO_2	Measured CO_2 increase†	2.3 ± 0.3
F	Fossil-fuel CO_2 source‡	4.85 ± 0.32
H	Fossil-fuel O_2 sink from elements other than carbon§	2.01 ± 0.17
$F+H$	Total fossil-fuel O_2 sink§	6.86 ± 0.41
C	CO_2 source from cement manufacturing¶‡	0.12 ± 0.01
Derived quantities		
B	Net terrestrial carbon source¶‖	−0.2 ± 1.7
O	Net oceanic CO_2 sink¶	2.5 ± 1.7

* Derived by multiplying the total number of moles of O_2 in the atmosphere ($3.705\ 10^{19}$ (ref. 8)) by the coefficient ($b = -18.2$ per meg yr^{-1}) of the fitted curve to the La Jolla data in Fig. 1. The standard error in b estimated from the formal covariance matrix of the fit is ±1.8 per meg yr^{-1}, but we adopt an uncertainty of ±5 per meg yr^{-1} based on a subjective assessment of possible drift in the reference gases.

† Derived from the coefficient ($b = 1.25 \pm 0.14$ p.p.m. yr^{-1}) of the curve fitted to the La Jolla CO_2 data in Fig. 1. The uncertainty in b is estimated from the formal covariance matrix of the fit assuming that the standard error in individual data points is equal to the mean square of the residuals to the fit.

‡ Using CO_2 production figures for 1989 from ref. 23.

§ From ref. 8 using fossil-fuel production figures for 1989 from ref. 23.

‖ Derived using $B = -(1/\alpha_B)(\Delta O_2 + F + H)$ from equation (5) using $\alpha_B = 1.05$ (ref. 8).

¶ Derived using equation (5).

Adding equations (4) and (5) and solving for O yields

$$O = -(\Delta O_2 + H) - (\Delta CO_2 - C) - (\alpha_B - 1)B \qquad (6)$$

The last term on the right-hand side of equation (6) can be evaluated by solving equation (5) for B, although this term is virtually negligible as $\alpha_B \approx 1$.

Once sufficiently long time series for oxygen are available, it will be possible to estimate oceanic uptake of CO_2 using equation (6). Although the existing records are too short to yield definitive results, we can nevertheless use these data to illustrate the method. We have estimated (Table 2) the terms in equations (4) to (6) using the data from La Jolla to estimate global trends in O_2 and CO_2. The global O_2 depletion rate inferred from the La Jolla data agrees well with the trend expected from the burning of fossil fuels, implying that the net terrestrial carbon source is zero within the uncertainties. The data suggest that the oceans were a sink of $2.5 \pm 1.7 \times 10^{14}$ mol C yr^{-1} (3.0 ± 2.0 Gt C yr^{-1}) over the period from 1989 to 1991. This estimate of the oceanic sink agrees, within rather wide error margins, with estimates derived from ocean models calibrated with bomb ^{14}C data[1]. The largest uncertainties in the estimated oceanic uptake are contributed by the trend in O_2/N_2, and this uncertainty will decrease as longer time series are obtained.

Accurate determination of the O_2 depletion rate from measurement time series will require very stable standards. In this respect the present procedure, which relies on the stability of O_2/N_2 in compressed air cylinders, may not be adequate. To insure against the possibility of parallel drift in O_2/N_2 in reference cylinders, new methods of absolute standardization of O_2/N_2 mixtures are needed. □

Received 13 May; accepted 23 July 1992.

1. Keeling, C. D. *et al.* in *Aspects of Climate Variability in the Pacific and the Western Americas, Geophys. Monogr. 55* (ed. Peterson, D. H.) 165–236 (American Geophysical Union, Washington DC, 1989).
2. Tans, P. P., Fung, I. Y. & Takahashi, T. *Science* **247**, 1431–1438 (1990).
3. Broecker, W. S. & Peng, T.-H. *Tracers in the Sea* (Lamont-Doherty Geological Observatory, New York, 1982).

4. Liss, P. S. & Merlivat, L. in *The Role of Air–Sea Exchange in Geochemical Cycling* (ed. P. Buat-Menard) 113–127 (Reidel, Dordrecht, 1986).
5. Keeling, R. F., Bender, M. M., Najjar, R. G. & Tans, P. P. *Glob. biogeochem. Cycles* (submitted).
6. Benedict, F. G. *The Composition of the Atmosphere with Special Reference to its Oxygen Content* (Carnegie Institution of Washington, Washington DC, 1912).
7. Machta, L. & Hughes, E. *Science* **168,** 1582–1584 (1970).
8. Keeling, R. F. thesis, Harvard Univ. (1988).
9. Keeling, R. F. *J. atmos. Chem.* **7,** 153–176 (1988).
10. Broecker, W. S. *Science* **168,** 1537–1538 (1970).
11. Heimann, M., Keeling, C. D. & Tucker, C. J. in *Aspects of Climate Variability in the Pacific and the Western Americas, Geophys. Monogr. 55* (ed. Peterson, D. H.) 277–303 (American Geophysical Union, Washington DC, 1989).
12. Jenkins, W. J. & Goldman, J. C. *J. mar. Res.* **43,** 465–491 (1985).
13. Takahashi, T., Goddard, J., Chipman, D. W., Sutherland, S. C. & Mathieu, G. *Final Tech. Rep. to DOE under contract 19X-SC428C,* 1–111 (Lamont Doherty Geological Observatory, New York, 1991).
14. Tans, P. P., Conway, T. J. & Nakazawa, T. *J. geophys. Res.* **94,** 5151–5172 (1989).
15. Dugdale, R. C. & Goering, J. J. *Limnol. Oceanogr.* **23,** 196–206 (1967).
16. Emerson, S. *J. geophys. Res.* **92,** 6535–6544 (1987).
17. Laws, E. A. *Deep-Sea Res.* **38,** 143–167 (1991).
18. Eppley, R. & Peterson, B. J. *Nature* **282,** 677–680 (1979).
19. Martin, J. M., Knauer, G. A., Karl, D. M. & Broenkow, W. W. *Deep-Sea Res.* **34,** 267–285 (1987).
20. Najjar, R. G. Sarmiento, J. L. & Toggweiler, J. R. *Glob. biogeochem. Cycles* **6,** 45–76 (1992).
21. Samuels, B. L. & Cox, M. *Ocean Model.* **75,** 1–3 (1987).
22. Weiss, R. F. *Deep-Sea Res.* **17,** 721–735 (1970).
23. Marland, G. & Boden, T. in *Trends 91: A Compendium of Data on Global Change, ORNL/CDIAC-46* (eds Boden, T. A., Sepanski, R. J. & Stoss, F. W.) **389** (CDIAC, Oak Ridge Tennessee, 1991).
24. Peng, T. H., Takahashi, T., Broecker, W. S. & Olafsson, J. *Tellus* B**39,** 439–458 (1987).
25. Asper, V. L., Deuser, W. G., Knauer, G. A. & Lohernz, S. E. *Nature* **357,** 670–672 (1992).

ACKNOWLEDGEMENTS. We thank N. Trivet and V. Chorney of the Canadian Baseline Program, R. Francey of CSIRO, S. Wilson and L. Porter of the Cape Grim Baseline Air Pollution Station, and C. D. Keeling, A. Bollenbacher and D. Moss of the Scripps Institution of Oceanography for help with sampling; J. Anderson, P. McKinney and J. Firor for support; E. Atlas, D. Erickson, R. Najjar, M. Bender and U. Siegenthaler for helpful comments; and A. Manning for help with the figures. This work was supported by the US NSF; additional support for R.K. was provided by a postdoctoral fellowship in the Advanced Study Program at NCAR.